11-18-2022

Genetic code expansion in *Pseudomonas putida* KT2440

Xinyuan He

Tian Gao

Yan Chen

Kun Liu

Jiantao Guo

See next page for additional authors

Authors

Xinyuan He, Tian Gao, Yan Chen, Kun Liu, Jiantao Guo, and Wei Niu

HHS Public Access

Author manuscript

ACS Synth Biol. Author manuscript; available in PMC 2023 November 18.

Published in final edited form as:

ACS Synth Biol. 2022 November 18; 11(11): 3724–3732. doi:10.1021/acssynbio.2c00325.

Genetic code expansion in *Pseudomonas putida* KT2440

Xinyuan He[1], **Tianyu Gao**[2], **Yan Chen**[2], **Kun Liu**[2], **Jiantao Guo**[2,3,*], **Wei Niu**[1,3,*]

[1]Department of Chemical & Biomolecular Engineering, University of Nebraska-Lincoln, Lincoln, Nebraska, 68588, United States.

[2]Department of Chemistry, University of Nebraska-Lincoln, Lincoln, Nebraska, 68588, United States.

[3]The Nebraska Center for Integrated Biomolecular Communication (NCIBC), University of Nebraska-Lincoln, Lincoln, Nebraska, 68588, United States.

Abstract

Pseudomonas putida KT2440 is an emerging microbial chassis for bio-based chemical production from renewable feedstocks and environmental bioremediation. However, tools for studying, engineering, and modulating protein complexes and biosynthetic enzymes in this organism are largely underdeveloped. Genetic code expansion for the incorporation of unnatural amino acids (unAAs) into proteins can advance such efforts and, furthermore, enable additional controls of biological processes of the strain. In this work, we established the orthogonality of two widely used archaeal tRNA synthetase and tRNA pairs in KT2440. Following the optimization of decoding systems, four unAAs were incorporated into proteins in response to a UAG stop codon at 34.6-78% efficiency. In addition, we demonstrated the utility of genetic code expansion through the incorporation of a photocrosslinking amino acid, *p*-benzoyl-L-phenylalanine (pBpa), into glutathione *S*-transferase (GstA) and a chemosensory response regulator (CheY) for protein-protein interaction studies in KT2440. This work reported the successful genetic code expansion in KT2440 for the first time. Given the diverse structure and functions of unAAs that have been added to protein syntheses using the archaeal systems, our research lays down a solid foundation for future work to study and enhance the biological functions of KT2440.

Keywords

genetic code expansion; unnatural amino acids; Pseudomonas putida KT2440; photocrosslinking; protein-protein interactions

INTRODUCTION

Genetic code expansion is a powerful tool in synthetic biology to enable new biological functions for both fundamental studies and practical applications.[1-4] Adding unnatural

*To whom correspondence should be addressed: wniu2@unl.edu, jguo4@unl.edu.

Author Contributions

W.N. and J.G. conceived and supervised the study. X.H. and Y.C. performed the experiments and analyzed the data. All authors contributed to the writing and revision of the manuscript.

The authors declare no competing financial interest.

amino acids (unAAs) to the protein alphabet of a host cell entails the introduction of an orthogonal aminoacyl-tRNA synthetase (aaRS)/tRNA pair for site-specific incorporation in response to a blank codon, often the UAG amber stop codon (Figure 1A). In the past 20 years, more than 200 unAAs with diverse chemical properties have been genetically encoded into proteins of interest in virus, bacteria, yeasts, mammalian cells and even whole animals.[1-4] Applications in bacterial hosts mainly focused on two sets of aaRS/tRNA system that originated from archaea. The *Methanococcus jannaschii* tyrosyl-tRNA synthetase and $tRNA^{Tyr}_{CUA}$ (*Mj*TyrRS/tRNA) pair was the first pair explored for live-cell genetic code expansion with tyrosine analogs.[5] The discovery of natural decoding of the amber codon with pyrrolysine in *Methanosarcina barkeri* led to the use of the pyrrolysyl-tRNA synthetase and $tRNA^{Pyl}_{CUA}$ (*Mb*PylRS/PylT) pair for the incorporation of primarily lysine analogs.[6-10] The natural orthogonality of the two systems further allows the simultaneous encoding of two unAAs in response to two blank codons.[11, 12] The initial method development almost exclusively used *Escherichia coli* strains for the directed evolution of orthogonal aaRS/tRNA pairs.[2, 5] Currently, genetic code expansion has been implemented in more than 20 non-*E. coli* bacterial species with diverse biotechnological and biomedical interests for bioremediation, biomanufacturing, and fundamental research.[13-22]

In this work, we demonstrated the first effort for genetic code expansion in *Pseudomonas putida* KT2440 (KT2440), which is an emerging biotechnological chassis due to its diverse metabolic capability, genetic tractability, and readily available toolsets. A previous report has shown the utility of an engineered *Mb*PylRS/PylT system in *Pseudomonas aeruginosa* for the study of its pathogenicity.[19] In comparison, KT2440 lacks virulence factors and has the FDA HV1 certified status.[23] It recently attracted intense research interests as a host strain for sustainable chemical production, e.g., from lignin-derived carbon source, and for removal of environmental pollutants.[24-30] In order to fully realize the potential of KT2440 in biotechnological applications, new and robust tools are desirable to further characterize, engineer, and control the functions of protein complexes and biosynthetic enzymes in this organism. Here, we successfully established both the *Mj*TyrRS/tRNA and the *Mb*PylRS/PylT systems in KT2440 through the demonstration of site-specific incorporations of four unAAs (Figure 1B) in superfolder green fluorescent protein (sfGFP). We further showed the utility of genetic code expansion in KT2440 through the incorporation of *p*-benzoyl-L-phenylalanine (pBpa), a photocrosslinker, for protein-protein interaction studies.

RESULTS and DISCUSSIONS

Genetic code expansion using the *Mj*TyrRS/tRNA pair

To establish the *M. jannaschii* tyrosyl-tRNA synthetase/$tRNA^{Tyr}_{CUA}$ (*Mj*TyrRS/tRNA) system in KT2440, we chose the incorporation of *p*-azido-L-phenylalanine (pAzF) as a proof of concept. pAzF contains an azide group that is broadly applied to protein labeling through bioorthogonal reactions, crosslinking, and structural studies.[31-33] Furthermore, due to the high specificity of the *Mj*TyrRS-derived pAzF tRNA synthetase (AzFRS), genetic encoding of pAzF has been used as a model system for genetic code expansion in various bacterial species.[13, 16, 17, 21, 22]

Here, we adopted a plasmid-based system for codon expansion in KT2440. Three broad-host-range (BHR) cloning vectors of different yet compatible replication origins were selected for this purpose.[34, 35] The rationale of examining plasmids with different copy numbers is to optimize the expression of amber suppression machinery while maintain healthy cell growth. One general concern of codon expansion is whether the introduction of the suppression system interferes with normal cellular activities. Previous studies, in both prokaryotic and eukaryotic cells, showed minimal[36-38] to detectable[39] level of fitness changes. To gauge the relative copy number of the three vectors in KT2440, a wild-type superfolder green fluorescent protein (sfGFP) was expressed under the P_{tac} promoter from these vectors. A stepwise increase in cellular fluorescence of approximately threefold was observed when the vector was changed from pSEVA621 (RK2 *ori*) to pSEVA651 (RFS1010 *ori*), and from pSEVA651 to pBBRMCS2 (pBBR *ori*) (Figure S1).

We first examined the orthogonality of the *Mj*TyrRS/tRNA pair to the endogenous translational machinery in KT2440. Plasmid pBBR-sfGFP N149TAG was constructed by cloning a sfGFP gene with an amber codon at the permissive site of N149 behind the P_{tac} promoter in vector pBBRMCS2. This base plasmid was then used to build two additional plasmids, which either expressed an evolved AzFRS[31] from the same gene cassette with the mutant sfGFP or expressed the *Mj*tRNA under the control of an *E. coli*-derived Prok promoter (Figure S2A). The three plasmids were individually transformed into KT2440 to evaluate the sfGFP expression. Taken the fluorescence level in cells containing the pBBR-sfGFP N149TAG plasmid as the background, no statistically significant change in fluorescence ($p > 0.05$) was observed in cells expressing just the *Mj*tRNA, or the AzFRS (Figure S2B). The observation showed that both the aminoacylation of the *Mj*tRNA by endogenous aaRSs and the aminoacylation of endogenous tRNA by AzFRS was low, which resulted in levels of amber suppression that were comparable to the host's natural ability. The *Mj*TyrRS/tRNA pair therefore was considered orthogonal in KT2440.

Genetic incorporation of pAzF was examined and optimized by tuning the expression level of AzFRS through controlling its gene copy using the three BHR vectors (Figure 2A). The efficiency of decoding an amber codon at the N149 position in sfGFP was used to gauge the incorporation. When vector pBBRMCS2 was used, a single plasmid that encoded AzFRS, sfGFP N149TAG and *Mj*tRNA was constructed (Figure 2A). When vector pSEVA621 or pSEVA651 was used, obtained AzFRS-encoding plasmid was paired with pBBR-sfGFP N149TAG-*Mj*tRNA (Figure 2A) to achieve the simultaneous delivery of all three genetic components. However, both the transformation of the pBBR-derived single plasmid and the co-transformation of pBBR-sfGFP N149TAG-*Mj*tRNA together with pSEVA651-AzFRS into the KT2440 strain led to low efficiency, slow growth (i.e., delayed colony formation), and ununiformed colony sizes. Characterization of these transformants further showed inconsistent sfGFP expression (Figure S3). Since normal cell growth was observed when either the AzFRS or the *Mj*tRNA was overexpressed, the observation indicated that high-level co-expression of AzFRS and *Mj*tRNA likely contributed to the growth defect. Meanwhile, normal transformation efficiency and healthy growth were observed when KT2440 was co-transformed with pBBR-sfGFP N149TAG-*Mj*tRNA and pSEVA621-AzFRS. Obtained clones were cultured to evaluate the incorporation of pAzF into sfGFP. With a low background of fluorescence in the absence of pAzF, an approximate

8.8-fold higher sfGFP expression was detected in the presence of 1 mM pAzF (Figure 2B). The level of sfGFP expression accounted for a 78.4% incorporation efficiency in comparison to the expression of the wild-type sfGFP from the pBBRMCS2 vector under the same cultivation condition (Figure S1B). The expressed sfGFP was subsequently purified (Figure S4A) and analyzed by tandem mass spectrometry (MS/MS). The peptide fragment that covered position 149 in sfGFP, i.e., LEYNFNSH(F+41)VYITADK, has a F+41 modification at the intended incorporation site. The modification corresponded to the molecular weight of pAzF (Figure S4B). The MS result confirmed the site-specific incorporation of pAzF into sfGFP in KT2440.

We further validated the established genetic system for the *Mj*TyrRS/tRNA pair through the genetic code expansion of *p*-benzoyl-L-phenylalanine (pBpa) in KT2440. pBpa was mainly used as a photocrosslinker to detect the interaction between a protein and its binding partners.[18, 40] An *Mj*TyrRS-derived tRNA synthetase for pBpa (BpaRS) has been applied to expand the genetic code in various bacteria.[40] To enable the incorporation of pBpa in KT2440, the AzFRS in pSEVA621-AzFRS was replaced with BpaRS. The obtained plasmid was co-transformed with pBBR-sfGFP N149TAG-*Mj*tRNA into KT2440 for evaluating the cellular fluorescence. When pBpa was provided at 1 mM in the culture media, a 4.9-fold increase in the fluorescence intensity of sfGFP was detected (Figure 2B), which corresponded to a 45.4% incorporation efficiency (Figure S1B). MS/MS analysis of purified sfGFP further confirmed the incorporation of pBpa. As shown in Figure S5, the peptide fragment covering the incorporation site, i.e., LEYNFNSH(F+104)VYITADK, contained a residue with molecular weight of pBpa at position 149. Furthermore, when either pAzF or pBpa was included in the culture media, no mis-incorporation of natural amino acids was identified. Overall, an approach to site-specifically incorporate pAzF and pBpa into sfGFP using variants of the *Mj*TyrRS/tRNA pair in *P. putida* KT2440 was established with high efficiency and fidelity.

Genetic code expansion using the *Mb*PylRS/PylT pair

The readily accessible N^{ε}-(tert-butoxycarbonyl)-L-lysine (BocK) was chosen as a model compound to establish the genetic code expansion with the *Mb*PylRS/PylT pair in KT2440. A reported *Mb*PylRS mutant (PylRS*, Y349F) with good activity towards BocK was used in this effort.[8] We first evaluated the orthogonality of the *Mb*PylRS/PylT pair to the host's endogenous system using a similar approach to the evaluation of the *Mj*TyrRS/tRNA pair (Figure S6). Besides plasmid pBBR-sfGFP N149TAG, which was used to gauge the background amber suppression in the host strain, one plasmid expressing the PylRS* (pBBR-PylRS*-sfGFP N149TAG) and one plasmid expressing the PylT (pBBR-sfGFP N149TAG-Plpp-PylT) were constructed for the experiment (Figure S6). When each plasmid was individually transformed into KT2440, no significant difference in cellular fluorescence was detected. The observation showed that the *Mb*PylRS/PylT pair is also orthogonal in KT2440.

Following the steps taken to optimize the genetic system for the genetic code expansion with the *Mj*TyrRS/tRNA pair, the effect of PylRS* expression level was examined by cloning the encoding gene into the three BHR vectors. Again, normal transformation and

healthy cell growth were only observed when the tRNA synthetase was expressed from the pSEVA621 vector, which has the lowest relative copy number in KT2440 (Figure S1). Cells co-transformed with pBBR-sfGFP N149TAG-Plpp-PylT and pSEVA621-PylRS* showed a 23.5-fold increase in fluorescence when BocK was included at 1 mM in the culture media (Figure 3B). Although the results demonstrated an initial success of implementing the *Mb*PylRS/PylT pair, the normalized fluorescence value only represented a 14.4% incorporation efficiency, which was substantially lower than what was observed using the *Mj*TyrRS/tRNA pair (Figure 2B).

Since the expression of tRNA was identified as a critical factor in decoding efficiency, we next focused on testing different promoters for PylT. The initial system had an *E. coli lpp* promoter, which was commonly used in the genetic code expansion with the *Mb*PylRS/PylT pair.[7-9] Meanwhile, its strength in KT2440 is unknown. To identify alternate tRNA promoters, we analyzed an RNA-seq dataset[41] for the expression level of endogenous tRNAs when KT2440 cells were cultured to the exponential growth phase. The two tRNAs with the highest expression level were a Tyr tRNA (PP_t01) and a Leu tRNA (PP_t68). Therefore, we constructed two new plasmids by replacing the *lpp* promoter on pBBR-sfGFP N149TAG-Plpp-PylT with the promoters of the above tRNAs. A third plasmid was built with the Prok promoter that was used for the expression of the *M. jannaschii* tyrosyl-tRNA. Together with plasmid pSEVA621-PylRS*, we examined the expression of sfGFP N149TAG in KT2440. All three promoters led to higher fluorescence than the *lpp* promoter. The highest expression was observed when the promoter for the Tyr tRNA (P_t01) was used. A 34.6% decoding efficiency was achieved (Figure 3B). MS/MS analysis of purified sfGFP 149BocK identified a lysine residue at the intended incorporation site, i.e., position 149, instead of BocK (Figure S7B). It corresponded to the loss of the *tert*-butoxycarbonyl group due to the instability of the carbamate bond under the tandem MS condition, which was an observation reported previously.[42-44] Further MS analysis of the full-length purified protein confirmed the incorporation of BocK. A single monoisotopic mass signal of 27386.7 Da was identified, which corresponds to sfGFP with BocK following the loss of N-terminal Met (expected mass 27386.7 Da, Figure S7C). Together with the low background of sfGFP expression in the absence of BocK (Figure 3B), the MS analysis confirmed the site-specific incorporation of BocK.

The established genetic system for the *Mb*PylRS/PylT pair was also applied to the incorporation of N^{ε}-(4-pentynyloxycarbonyl)-L-lysine (AlkK, Figure 1) in KT2440. AlkK contained an alkyne group that has been used as a chemical handle for protein labelling.[45-47] A previously reported *Mb*PylRS variant (AlkKRS) was used in this experiment.[48] Plasmids pSEVA621-AlkKRS and pBBR-sfGFP N149TAG-P_t01-PylT was co-transformed into KT2440 and the expression of sfGFP was monitored. With minimal background signal, a 73.1-fold increase in fluorescence was observed when cells were cultured in the presence of 1 mM AlkK (Figure 3B). The incorporation efficiency was calculated as 53.7%. Peptides with AlkK or Lys at position 149 were identified in MS/MS analysis, which again indicated the cleavage of the carbamate bond (Figure S8). In the presence of BocK or AlkK, no natural amino acid other than lysine was detected at the designed incorporation site. Therefore, both unAAs were site-specifically incorporated at high efficiency and fidelity in KT2440.

Protein-protein interaction studies using pBpa

Biomolecular interactions dictate cellular processes. However, due to the weak and/or transient nature, identifying the interacting partners is often challenging.[49, 50] Building upon our success of genetic code expansion in KT2440, we explored the utility of the method to study protein-protein interactions in this strain through the incorporation of pBpa, which has been applied to probe protein interactions in bacterial and mammalian cells (Figure 4A).[40, 51] As a proof-of-concept, we first studied the glutathione *S*-transferase protein (GstA, PP_1162) in KT2440. Bacterial GSTs function in detoxification pathways and protect cells from oxidative stresses.[52] Current structural studies indicate that bacterial GSTs form homodimers. To verify the possible dimer formation of the GstA in KT2440, we first built a homology model of the protein in MODELLER (Figure S9A).[53] Residue Phe53 which resides in a flexible region at the interface of the two monomers was chosen as a permissive position for pBpa incorporation.[40] The corresponding codon was mutated into the amber codon and the resulting gene was expressed together with BpaRS and *Mj*tRNA in KT2440 in the presence of 1 mM pBpa. Homodimer formation was first investigated *in vitro* using purified GstA 53pBpa protein. Following irradiation at 360 nm for 30 min, western blot showed a new band with a molecular weight close to 50 kDa (lane 2, Figure 4B), which corresponded to the homodimer of a GstA with a 6xHis tag (a 23.8 kDa protein). Meanwhile, the same treatment did not result in new protein band for the control sample of the wild-type GstA (lane 1, Figure 4B). We further examined the oligomeric state of GstA under the natural biological environment. KT440 cells expressing either the wild-type GstA or the GstA 53pBpa mutant were exposed to UV irradiation followed by cell lysis and western blot analysis. Again, homodimer formation was only observed in the lysate of irradiated cells expressing GstA 53pBpa (lanes 7 and 8, Figure 4B) not the wild-type GstA (lane 4 and 5, Figure 4B). The absence of dimer prior to UV irradiation further confirmed the crosslinking was initiated by UV activation of the pBpa (lane 6, Figure 4B). Above results showed that the GstA of KT2440 strain also forms homodimer both *in vitro* and *in vivo*. Further analysis of the wild-type and the pBpa-containing GstA proteins under native PAGE conditions confirmed this conclusion (Figure S9B). It also demonstrated that the incorporation of pBpa at position 53 of GstA did not affect the formation of homodimer (Figure S9B). We did observe additional bands other than the dimer of GstA following the photocrosslinking. This could be caused by side reactions of the highly reactive radical species formed by the benzophenone moiety in pBpa after photoactivation. The effect can be exacerbated by high concentrations of GstA 53pBpa under crosslinking conditions. Similar observations were reported by others.[40]

We next applied the pBpa incorporation to investigate protein interaction events in signal transduction processes in KT2440. Bacterial two-component system consists of a histidine kinase (HK) and its cognate response regulator (RR). They play the primary role of sensing and adaptation to environmental changes.[54] Here, we examined interacting partners of the CheY (PP_4340) protein, which is a chemosensory response regulator in chemotaxis. It is activated through the phosphorylation by the upstream HK, CheA (PP_4338).[55] To select permissive positions for the incorporation of pBpa, we focused on the interacting surface between CheY and CheA proteins. Based on the crystal structure of *Thermotoga maritima* CheY in complex with CheA (PDB ID: 1U0S), two residues, i.e., Ile90 and Phe100 that

correspond to Ile91 and Tyr101 in CheY of KT2440 (Figure S10), were chosen. An Amber mutation was individually introduced at each site and the mutant gene was co-expressed with BpaRS and *Mj*tRNA in KT2440 cultured in the presence of 1 mM pBpa. Following irradiation, cells were harvested and crosslinking products together with unreacted CheY 91pBpa or CheY 101pBpa were purified by affinity resins. SDS-PAGE analysis revealed new bands with significant intensity in each sample (Fig. 4C). Two bands (Band 1 and Band 2) between 25 and 37 kDa (lane 4, Figure 4C) were identified in irradiated cells expressing CheY 91pBpa. One band of similar molecular weight to Band 1 (Band 3) and one band of around 75 kDa (Band 4) were observed in cells expressing CheY 101pBpa. Results of western blot further confirmed that these bands were formed by proteins with His tag (Fig. 4D). At the higher detection sensitivity, a band of similar molecular weight to Band 4 was also purified from cells expressing CheY 91pBpa (Band 4') and a band of similar molecular weight to Band 2 was also detected in cells with CheY 101pBpa (Band 2'). The observation indicated that major photocrosslinking events of CheY mutants were not biased by the position of pBpa incorporation. Bands 2, 3, and 4 were submitted for proteomics analysis to identify crosslinked protein species (Table S3 and S4). Peptides of CheY had the highest abundance in all samples, which verified that the formation of new protein bands was driven by the incorporated pBpa. Majority of the proteins identified in bands of lower molecular weights were known for high intracellular concentrations in bacteria, such as ribosomal proteins and enzymes for fatty acid biosynthesis (Table S3).[56] A Similar trend was observed for the band around 75 kDa. Besides CheY, top results included chaperons and transcription/translation elongation factors (Table S4), which were shown to be highly abundant in proteomics studies.[56] It is unlikely that these proteins function in chemotaxis through the interaction with CheY. We hypothesize that the background signals were caused by nonspecific crosslinking reactions that were partially promoted by high-level expression of CheY. Meanwhile, CheA was successfully identified in Band 4. The result confirmed that the CheY/CheA interaction in KT2440 and validated the photocrosslinking approach. In addition, a chemoreceptor protein, McpQ (PP_5020), which responds to citrate/metal ion complexes was observed in Band 4 (Table S4).[57] Possible interaction between CheA and McpQ has been indicated in the mode of chemotaxis events.[57] Further study is needed to verify possible direct interaction between CheY and McpQ.

SUMMARY and FUTURE WORKS

In this work, we successfully established the *M. jannaschii* tyrosyl-tRNA synthetase and $tRNA^{Tyr}_{CUA}$ (*Mj*TyrRS/tRNA) and the *M. barkeri* pyrrolysyl-tRNA synthetase and $tRNA^{Pyl}_{CUA}$ (*Mb*PylRS/PylT) systems for the genetic codon expansion in *P. putida* KT2440. Tuning the expression levels of tRNA synthetase and tRNA led to the incorporation of four unAAs (pAzF, pBpa, BocK, and AlkK) into sfGFP at high efficiencies (34.6%-78%). All previously engineered aaRSs that are derived from *Mj*TyrRS and *Mb*PylRS can now be readily applied to genetic code expansion in KT2440. We further demonstrated the utility of the methodology by detecting protein interactions through the incorporation of a photocrosslinker unAA into GstA and CheY proteins. The successful genetic code expansion in KT2440 adds new gadgets to the synthetic biology toolkit of this biotechnologically important strain and augments its biological function. Further application

of the approach can be facilitated by generating fully or partially genomic recoded KT2440 variants, in which all the amber codons or ones in genes encoding essential functions are replaced with alternate stop codon in order to minimize disturbance to cells' normal physiological activities due to unwanted suppression events.[58-60]

MATERIALS AND METHODS

Reagents and media.

All commercial chemicals are of reagent grade or higher. All solutions were prepared in deionized water that was further treated by Barnstead Nanopure® ultrapure water purification system (Thermo Fisher Scientific). *Pseudomonas putida* KT2440 was obtained from the American Type Culture Collection (ATCC 47054). The strain was routinely cultured at 30 °C on LB agar plates or in LB liquid medium. Antibiotics were added where appropriate to following final concentrations: gentamicin (10 mg/L), kanamycin (50 mg/L), ampicillin (100 mg/L), chloramphenicol (25 mg/L). *p*-Azido-L-phenylalanine (pAzF), *p*-benzoyl-L-phenylalanine (pBpa), and N^{ε}-3-(tert-butyloxycarbonyl)-L-lysine (BocK) were purchased from Bachem. N^{ε}-(4-pentynyloxycarbonyl)-L-lysine (AlkK) was synthesized by following previously published procedure.[48] unAAs were dissolved in 1 M NaOH to make stock solutions. The pH values of culture media were adjusted to 7.0 before use. Solutions of antibiotics and unAAs were filtered through 0.22 μm sterile membrane filters.

Plasmid construction.

E. coli GeneHogs (Thermo Fisher Scientific) or *E. coli* NEB 5-alpha (New England Biolabs) was used for routine cloning and plasmid propagation. Plasmid construction was performed using T4 DNA ligase (Thermo Fisher Scientific) or Gibson Assembly method.[61] Genomic DNA of *P. putida* KT2440 was isolated using the PureLink™ genomic DNA mini kit (Thermo Fisher Scientific). PCR amplifications were carried out using KOD Hot Start DNA polymerase (Millipore Sigma) by following manufacturer's protocol. Restriction enzymes were purchased from New England Biolabs. Primer synthesis and DNA sequencing services were provided by Eurofins MWG Operon. Primers used in this study are listed in Table S1. Plasmids used in this study are listed in Table S2. Details of plasmid construction are included in the Supplemental Information.

Fluorescence measurement of *P. putida* KT2440 culture.

Transformed *P. putida* KT2440 cells were grown in 5 mL LB media containing appropriate antibiotics at 30 °C with agitation at 250 rpm. When the cell density reached an OD_{600} of 0.4, unAA was supplemented in the culture media at the indicated concentration. Following 12 h of cultivation, cells were harvested, washed with PBS for three times, then resuspended in PBS for cell density measurement and fluorescence quantification (excitation at 485 nm, emission at 528 nm) using a Biotek Synergy HTX plate reader. Normalized fluorescence was calculated by dividing the absolute fluorescence by cell density. The incorporation efficiency was calculated by dividing the normalized fluorescence of cells expressing the unAA-containing sfGFP by the normalized fluorescence of cells expressing the wild-type sfGFP from the pBBRMCS2 vector under the same cultivation condition.

Purifiaction and MS analysis of sfGFP variants.

For the analysis of unAA incorporation into sfGFP, a 50 mL cell culture was routinely grown under the same condition that was used for fluorescence measurement. Harvested cells were lysed and sfGFP was purified on Ni Sepharose 6 Fast Flow resin (GE Healthcare) following the manufacturer's protocol. Purified protein was quantified by Bradford assay and analyzed by SDS-PAGE. For tandem mass spectrometry analysis, bands corresponding to the size of sfGFP were collected and processed by the Proteomics and Metabolomics Facility of the Nebraska Center for Biotechnology at UNL. Following treatment with trypsin overnight at 37 °C, peptides were extracted from the gel pieces, dried down, and re-dissolved in 25 μL of an aqueous solution of acetonitrile (2.5%) and formic acid (0.1%). Each digest was run by an RSLCnano system using a 1 h gradient on a 0.075 mm x 250 mm C18 column feeding into a Q-Exactive HF mass spectrometer. MS/MS data was analyzed using Mascot, which was set up to search a database that was customized with the provided protein sequence. Mascot search has a fragment ion mass tolerance of 0.060 Da and a parent ion tolerance of 10.0 ppm. Scaffold was used to validate MS/MS-based peptide and protein identifications. Peptide identifications were accepted if they could be established at greater than 99.0% probability by the Peptide Prophet algorithm[62] with Scaffold delta-mass correction. Protein probabilities were assigned by the Protein Prophet algorithm.[63] For mass analysis of the full-length sfGFP 149BocK protein, the purified fraction was first dialyzed into phosphate buffer (100 mM, pH 7.4) to remove imidazole, then analyzed by the Proteomics and Metabolomics facility on a Q-Exactive HF mass spectrometer. The protein mass was calculated using the Protein Deconvolution software (ThermoFisher Scientific).

Photocrosslinking experiments.

To produce GstA or CheY protein containing pBpa, KT2440 was co-transformed with pSEVA621-BpaRS and pBBR-GstA F53TAG-*Mj*tRNA or pBBR-CheY I91TAG-*Mj*tRNA (or pBBR-CheY Y101TAG-*Mj*tRNA) and cultured in LB media with 1 mM pBpa. To produce wild-type proteins, pBBR-GstA-*Mj*tRNA or pBBR-CheY-*Mj*tRNA was transformed into KT2440. For photocrosslinking of purified protein, the wild-type or GstA 53pBpa was diluted to 1.0 mg/mL in irradiation buffer (25 mM potassium phosphate, pH 7.4), then aliquoted into a 96 well plate. Protein samples were irradiated at 360 nm for a total of 30 min with the samples cooled on ice for 5 min in every 10 min. Irradiated protein samples were analyzed by western blot. Briefly, proteins separated on an SDS-PAGE were transferred onto a nitrocellulose membrane, which was probed by a mouse anti-6xHis tag monoclonal antibody (MCA1396, Bio-Rad Laboratories), followed by HRP conjugated goat anti-mouse IgG (1706516, BioRad Laboratories). Blots were developed using the Opti-4CN detection kit (BioRad Laboratories) and imaged using a Gel Doc XR+ system. For photocrosslinking with intact cells, cells were harvest, washed, and resuspended in PBS buffer to an OD_{600nm} of 1.0. Following irradiation at 360 nm for 30 min with periodic cooling on ice every 10 min, cells were lysed either for western blot analysis or for proteins purification. To identify crosslinked protein with CheY, purified proteins were first separated on SDS-PAGE. Bands of crosslinking products (Figure 4C) were collected for proteomics analysis.

Supplementary Material

Refer to Web version on PubMed Central for supplementary material.

ACKNOWLEDGMENTS

This work was supported by Nebraska Center for Energy Science Research, the Nebraska Center for Integrated Biomolecular Communication (NIH National Institutes of General Medical Sciences P20 GM113126), and National Institute of Health (grant 1R01GM138623 to J.G. and W.N.). We thank the Proteomics & Metabolomics Facility (RRID:SCR_021314), Nebraska Center for Biotechnology at the University of Nebraska-Lincoln for the mass spectrometry analysis. The facility and instrumentation are supported by the Nebraska Research Initiative.

REFERENCES

1. Liu CC, and Schultz PG (2010) Adding new chemistries to the genetic code, Annu. Rev. Biochem 79, 413–444. [PubMed: 20307192]
2. Dumas A, Lercher L, Spicer CD, and Davis BG (2015) Designing logical codon reassignment - Expanding the chemistry in biology, Chem. Sci 6, 50–69. [PubMed: 28553457]
3. Young DD, and Schultz PG (2018) Playing with the Molecules of Life, ACS Chem. Biol 13, 854–870. [PubMed: 29345901]
4. de la Torre D, and Chin JW (2021) Reprogramming the genetic code, Nat. Rev. Genet 22, 169–184. [PubMed: 33318706]
5. Wang L, Brock A, Herberich B, and Schultz PG (2001) Expanding the genetic code of Escherichia coli, Science (Washington, DC, U. S.) 292, 498–500.
6. Srinivasan G, James CM, and Krzycki JA (2002) Pyrrolysine encoded by UAG in Archaea: charging of a UAG-decoding specialized tRNA, Science (Washington, DC, U. S.) 296, 1459–1462.
7. Neumann H, Peak-Chew SY, and Chin JW (2008) Genetically encoding Nε-acetyllysine in recombinant proteins, Nature Chemical Biology 4, 232–234. [PubMed: 18278036]
8. Yanagisawa T, Ishii R, Fukunaga R, Kobayashi T, Sakamoto K, and Yokoyama S (2008) Multistep Engineering of Pyrrolysyl-tRNA Synthetase to Genetically Encode Nε-(o-Azidobenzyloxycarbonyl) lysine for Site-Specific Protein Modification, Chemistry & Biology 15, 1187–1197. [PubMed: 19022179]
9. Chen PR, Groff D, Guo J, Ou W, Cellitti S, Geierstanger BH, and Schultz PG (2009) A facile system for encoding unnatural amino acids in mammalian cells, Angew. Chem., Int. Ed 48, 4052–4055.
10. Nozawa K, O'Donoghue P, Gundllapalli S, Araiso Y, Ishitani R, Umehara T, Soll D, and Nureki O (2009) Pyrrolysyl-tRNA synthetase-tRNAPyl structure reveals the molecular basis of orthogonality, Nature (London, U. K.) 457, 1163–1167. [PubMed: 19118381]
11. Neumann H, Wang K, Davis L, Garcia-Alai M, and Chin JW (2010) Encoding multiple unnatural amino acids via evolution of a quadruplet-decoding ribosome, Nature 464, 441–444. [PubMed: 20154731]
12. Hankore ED, Zhang L, Chen Y, Liu K, Niu W, and Guo J (2019) Genetic incorporation of noncanonical amino acids using two mutually orthogonal quadruplet codons, ACS Synth. Biol 8, 1168–1174. [PubMed: 30995842]
13. Wang F, Robbins S, Guo J, Shen W, and Schultz PG (2010) Genetic incorporation of unnatural amino acids into proteins in Mycobacterium tuberculosis, PLoS One 5.
14. Lin S, Zhang Z, Xu H, Li L, Chen S, Li J, Hao Z, and Chen PR (2011) Site-Specific Incorporation of Photo-Cross-Linker and Bioorthogonal Amino Acids into Enteric Bacterial Pathogens, J. Am. Chem. Soc 133, 20581–20587. [PubMed: 22084898]
15. Tack DS, Ellefson JW, Thyer R, Wang B, Gollihar J, Forster MT, and Ellington AD (2016) Addicting diverse bacteria to a noncanonical amino acid, Nat. Chem. Biol 12, 138–140. [PubMed: 26780407]
16. Gan Q, Lehman BP, Bobik TA, and Fan C (2016) Expanding the genetic code of Salmonella with non-canonical amino acids, Sci. Rep 6, 39920. [PubMed: 28008993]

17. He J, Van Treeck B, Nguyen HB, and Melancon CE (2016) Development of an Unnatural Amino Acid Incorporation System in the Actinobacterial Natural Product Producer Streptomyces venezuelae ATCC 15439, ACS Synth. Biol 5, 125–132. [PubMed: 26562751]

18. Takahashi H, Dohmae N, Kim KS, Shimuta K, Ohnishi M, Yokoyama S, and Yanagisawa T (2020) Genetic incorporation of non-canonical amino acid photocrosslinkers in Neisseria meningitidis: New method provides insights into the physiological function of the function-unknown NMB1345 protein, PLoS One 15, e0237883. [PubMed: 32866169]

19. Zheng H, Lin S, and Chen PR (2020) Genetically encoded protein labeling and crosslinking in living Pseudomonas aeruginosa, Bioorg. Med. Chem 28, 115545. [PubMed: 32503693]

20. Ozer E, Yaniv K, Chetrit E, Boyarski A, Meijler MM, Berkovich R, Kushmaro A, and Alfonta L (2021) An inside look at a biofilm: Pseudomonas aeruginosa flagella biotracking, Sci. Adv 7, eabg8581. [PubMed: 34117070]

21. Stork DA, Squyres GR, Kuru E, Gromek KA, Rittichier J, Jog A, Burton BM, Church GM, Garner EC, and Kunjapur AM (2021) Designing efficient genetic code expansion in Bacillus subtilis to gain biological insights, Nat. Commun 12, 5429. [PubMed: 34521822]

22. Gonzalez SS, Ad O, Shah B, Zhang Z, Zhang X, Chatterjee A, and Schepartz A (2021) Genetic Code Expansion in the Engineered Organism Vmax X2: High Yield and Exceptional Fidelity, ACS Cent. Sci 7, 1500–1507. [PubMed: 34584951]

23. Kampers LF, Volkers RJ, and Martins Dos Santos VA (2019) *Pseudomonas putida* KT 2440 is HV 1 certified, not GRAS, Microb. Biotechnol 12, 845–848. [PubMed: 31199068]

24. Nelson KE, Weinel C, Paulsen IT, Dodson RJ, Hilbert H, Martins dos Santos VAP, Fouts DE, Gill SR, Pop M, Holmes M, Brinkac L, Beanan M, DeBoy RT, Daugherty S, Kolonay J, Madupu R, Nelson W, White O, Peterson J, Khouri H, Hance I, Lee PC, Holtzapple E, Scanlan D, Tran K, Moazzez A, Utterback T, Rizzo M, Lee K, Kosack D, Moestl D, Wedler H, Lauber J, Stjepandic D, Hoheisel J, Straetz M, Heim S, Kiewitz C, Eisen J, Timmis KN, Dusterhoft A, Tummler B, and Fraser CM (2002) Complete genome sequence and comparative analysis of the metabolically versatile Pseudomonas putida KT2440, Environ. Microbiol 4, 799–808. [PubMed: 12534463]

25. Belda E, van Heck RGA, Jose Lopez-Sanchez M, Cruveiller S, Barbe V, Fraser C, Klenk H-P, Petersen J, Morgat A, Nikel PI, Vallenet D, Rouy Z, Sekowska A, Martins dos Santos VAP, de Lorenzo V, Danchin A, and Medigue C (2016) The revisited genome of Pseudomonas putida KT2440 enlightens its value as a robust metabolic chassis, Environ. Microbiol 18, 3403–3424. [PubMed: 26913973]

26. Beckham GT, Johnson CW, Karp EM, Salvachua D, and Vardon DR (2016) Opportunities and challenges in biological lignin valorization, Curr. Opin. Biotechnol 42, 40–53. [PubMed: 26974563]

27. Nikel PI, Chavarria M, Danchin A, and de Lorenzo V (2016) From dirt to industrial applications: *Pseudomonas putida* as a Synthetic Biology chassis for hosting harsh biochemical reactions, Curr. Opin. Chem. Biol 34, 20–29. [PubMed: 27239751]

28. Nikel PI, and de Lorenzo V (2018) *Pseudomonas putida* as a functional chassis for industrial biocatalysis: From native biochemistry to trans-metabolism, Metab. Eng 50, 142–155. [PubMed: 29758287]

29. Johnson CW, Salvachua D, Rorrer NA, Black BA, Vardon DR, St. John PC, Cleveland NS, Dominick G, Elmore JR, Grundl N, Khanna P, Martinez CR, Michener WE, Peterson DJ, Ramirez KJ, Singh P, VanderWall TA, Wilson AN, Yi X, Biddy MJ, Bomble YJ, Guss AM, and Beckham GT (2019) Innovative Chemicals and Materials from Bacterial Aromatic Catabolic Pathways, Joule 3, 1523–1537.

30. Niu W, Willett H, Mueller J, He X, Kramer L, Ma B, and Guo J (2020) Direct biosynthesis of adipic acid from lignin-derived aromatics using engineered Pseudomonas putida KT2440, Metab. Eng 59, 151–161. [PubMed: 32130971]

31. Chin JW, Santoro SW, Martin AB, King DS, Wang L, and Schultz PG (2002) Addition of p-Azido-L-phenylalanine to the Genetic Code of Escherichia coli, J. Am. Chem. Soc 124, 9026–9027. [PubMed: 12148987]

32. Ye S, Huber T, Vogel R, and Sakmar TP (2009) FTIR analysis of GPCR activation using azido probes, Nat. Chem. Biol 5, 397–399. [PubMed: 19396177]

33. Ye S, Zaitseva E, Caltabiano G, Schertler GFX, Sakmar TP, Deupi X, and Vogel R (2010) Tracking G-protein-coupled receptor activation using genetically encoded infrared probes, Nature (London, U. K.) 464, 1386–1389. [PubMed: 20383122]
34. Kovach ME, Phillips RW, Elzer PH, Roop RM II, and Peterson KM (1994) pBBR1MCS: a broad-host-range cloning vector, BioTechniques 16, 800,802. [PubMed: 8068328]
35. Martinez-Garcia E, Aparicio T, Goni-Moreno A, Fraile S, and de Lorenzo V (2015) SEVA 2.0: an update of the standard European vector architecture for de-/re-construction of bacterial functionalities, Nucleic Acids Res. 43, D1183–D1189. [PubMed: 25392407]
36. Elsasser SJ, Ernst RJ, Walker OS, and Chin JW (2016) Genetic code expansion in stable cell lines enables encoded chromatin modification, Nat. Methods 13, 158–164. [PubMed: 26727110]
37. Ernst RJ, Krogager TP, Maywood ES, Zanchi R, Ber'nek V. c., Elliott TS, Barry NP, Hastings MH, and Chin JW (2016) Genetic code expansion in the mouse brain, Nat. Chem. Biol 12, 776–778. [PubMed: 27571478]
38. Chen Y, Ma J, Lu W, Tian M, Thauvin M, Yuan C, Volovitch M, Wang Q, Holst J, Liu M, Vriz S, Ye S, Wang L, and Li D (2017) Heritable expansion of the genetic code in mouse and zebrafish, Cell Res 27, 294–297. [PubMed: 27934867]
39. Tack DS, Cole AC, Shroff R, Morrow BR, and Ellington AD (2018) Evolving Bacterial Fitness with an Expanded Genetic Code, Sci. Rep 8, 1–12. [PubMed: 29311619]
40. Chin JW, Martin AB, King DS, Wang L, and Schultz PG (2002) Addition of a photocrosslinking amino acid to the genetic code of Escherichia coli, Proc. Natl. Acad. Sci. U. S. A 99, 11020–11024. [PubMed: 12154230]
41. Lim HG, Rychel K, Sastry AV, Bentley GJ, Mueller J, Schindel HS, Larsen PE, Laible PD, Guss AM, Niu W, Johnson CW, Beckham GT, Feist AM, and Palsson BO (2022) Machine-learning from *Pseudomonas putida* KT2440 transcriptomes reveals its transcriptional regulatory network, Metab. Eng 72, 297–310. [PubMed: 35489688]
42. Schmied WH, Elsasser SJ, Uttamapinant C, and Chin JW (2014) Efficient multisite unnatural amino acid incorporation in mammalian cells via optimized Pyrrolysyl tRNA Synthetase/tRNA expression and engineered eRF1, J. Am. Chem. Soc 136, 15577–15583. [PubMed: 25350841]
43. Nguyen DP, Mahesh M, Elsasser SJ, Hancock SM, Uttamapinant C, and Chin JW (2014) Genetic Encoding of Photocaged Cysteine Allows Photoactivation of TEV Protease in Live Mammalian Cells, J. Am. Chem. Soc 136, 2240–2243. [PubMed: 24479649]
44. Chen Y, Ma B, Liu K, Gao T, Guo J, He X, Niu W, Niu W, and Guo J (2022) Noncanonical amino acid mutagenesis in response to recoding signal-enhanced quadruplet codons, Nucleic Acids Res.
45. Kolb HC, Finn MG, and Sharpless KB (2001) Click chemistry: diverse chemical function from a few good reactions, Angew. Chem., Int. Ed 40, 2004–2021.
46. Prescher JA, and Bertozzi CR (2005) Chemistry in living systems, Nat. Chem. Biol 1, 13–21. [PubMed: 16407987]
47. Lang K, and Chin JW (2014) Cellular Incorporation of Unnatural Amino Acids and Bioorthogonal Labeling of Proteins, Chem. Rev. (Washington, DC, U. S.) 114, 4764–4806.
48. Li Y, Pan M, Li Y, Huang Y, and Guo Q (2013) Thiol-yne radical reaction mediated site-specific protein labeling via genetic incorporation of an alkynyl-L-lysine analogue, Org. Biomol. Chem 11, 2624–2629. [PubMed: 23450369]
49. Hurley LH (2002) DNA and its associated processes as targets for cancer therapy, Nat. Rev. Cancer 2, 188–200. [PubMed: 11990855]
50. Wells JA, and McClendon CL (2007) Reaching for high-hanging fruit in drug discovery at protein-protein interfaces, Nature (London, U. K.) 450, 1001–1009. [PubMed: 18075579]
51. Hino N, Okazaki Y, Kobayashi T, Hayashi A, Sakamoto S, and Yokoyama S (2005) Protein photo-cross-linking in mammalian cells by site-specific incorporation of a photoreactive amino acid, Nat. Methods 2, 201–206. [PubMed: 15782189]
52. Allocati N, Federici L, Masulli M, and Di Ilio C (2009) Glutathione transferases in bacteria, FEBS J. 276, 58–75. [PubMed: 19016852]
53. Sali A, and Blundell TL (1993) Comparative protein modelling by satisfaction of spatial restraints, J Mol Biol 234, 779–815. [PubMed: 8254673]

54. Sourjik V, and Wingreen NS (2012) Responding to chemical gradients: bacterial chemotaxis, Curr. Opin. Cell Biol 24, 262–268. [PubMed: 22169400]

55. Wadhams GH, and Armitage JP (2004) Making sense of it all: Bacterial chemotaxis, Nat. Rev. Mol. Cell Biol 5, 1024–1037. [PubMed: 15573139]

56. Wang M, Herrmann CJ, Simonovic M, Szklarczyk D, and von Mering C (2015) Version 4.0 of PaxDb: Protein abundance data, integrated across model organisms, tissues, and cell-lines, Proteomics 15, 3163–3168. [PubMed: 25656970]

57. Martin-Mora D, Reyes-Darias J-A, Ortega A, Corral-Lugo A, Matilla MA, and Krell T (2016) McpQ is a specific citrate chemoreceptor that responds preferentially to citrate/metal ion complexes, Environ. Microbiol 18, 3284–3295. [PubMed: 26463109]

58. Lajoie MJ, Rovner AJ, Goodman DB, Aerni H-R, Haimovich AD, Kuznetsov G, Mercer JA, Wang HH, Carr PA, Mosberg JA, Rohland N, Schultz PG, Jacobson JM, Rinehart J, Church GM, and Isaacs FJ (2013) Genomically recoded organisms expand biological functions, Science 342, 357–360. [PubMed: 24136966]

59. Fredens J, Wang K, de la Torre D, Funke LFH, Robertson WE, Christova Y, Chia T, Schmied WH, Dunkelmann DL, Beranek V, Uttamapinant C, Llamazares AG, Elliott TS, and Chin JW (2019) Total synthesis of Escherichia coli with a recoded genome, Nature 569, 514–518. [PubMed: 31092918]

60. Asin-Garcia E, Martin-Pascual M, Garcia-Morales L, van Kranenburg R, and Martins dos Santos VAP (2021) ReScribe: An Unrestrained Tool Combining Multiplex Recombineering and Minimal-PAM ScCas9 for Genome Recoding Pseudomonas putida, ACS Synth. Biol 10, 2672–2688. [PubMed: 34547891]

61. Gibson DG, Young L, Chuang R-Y, Venter JC, Hutchison CA, and Smith HO (2009) Enzymatic assembly of DNA molecules up to several hundred kilobases, Nat. Methods 6, 343–345. [PubMed: 19363495]

62. Keller A, Nesvizhskii AI, Kolker E, and Aebersold R (2002) Empirical Statistical Model To Estimate the Accuracy of Peptide Identifications Made by MS/MS and Database Search, Anal. Chem 74, 5383–5392. [PubMed: 12403597]

63. Nesvizhskii AI, Keller A, Kolker E, and Aebersold R (2003) A Statistical Model for Identifying Proteins by Tandem Mass Spectrometry, Anal. Chem 75, 4646–4658. [PubMed: 14632076]

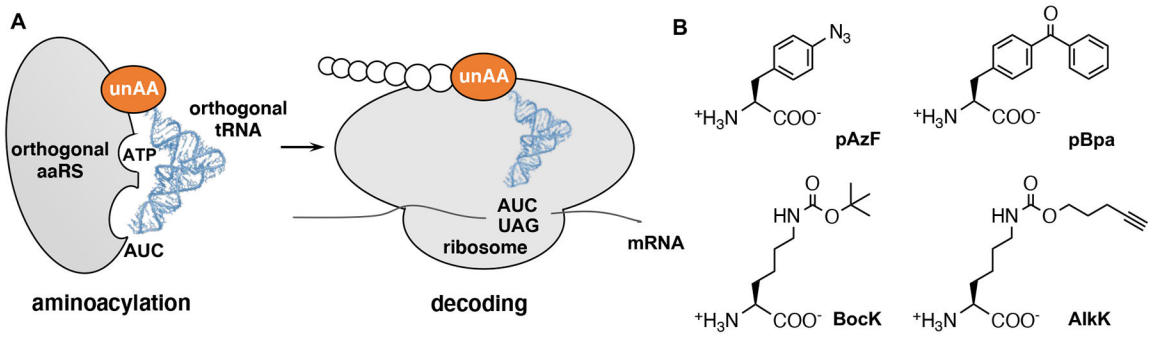

Figure 1.

A general scheme of genetic code expansion in KT2440. (A) An orthogonal aaRS/tRNA pair was efficiently expressed to genetically incorporate unAA into a protein of interest in response to an amber stop codon. (B) Structures of unAAs used in this study: *p*-azido-L-phenylalanine (pAzF), *p*-benzoyl-L-phenylalanine (pBpa), N^{ε}-(*tert*-butoxycarbonyl)-L-lysine (BocK), and N^{ε}-(4-pentynyloxycarbonyl)-L-lysine (AlkK).

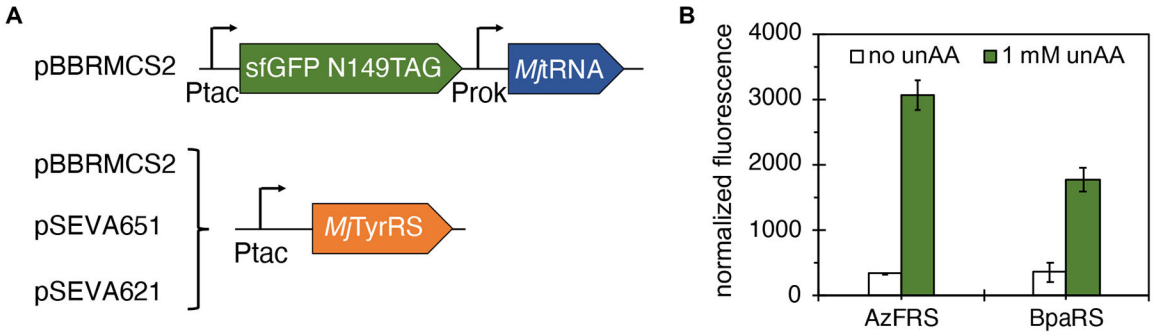

Figure 2. Genetic code expansion using the *Mj*TyrRS/tRNA pair in *P. putida* KT2440.

(A) Plasmid constructs for the expression of *Mj*tRNA and an unAA-specific *Mj*TyrRS variant. (B) Fluorescence of KT2440 cells co-transformed with pBBR-sfGFP N149TAG-*Mj*tRNA and pSEVA621-AzFRS or pSEVA621-BpaRS. Fluorescence intensity was normalized to cell growth. Data is plotted as the mean ± s.d. from n= 3 independent experiments.

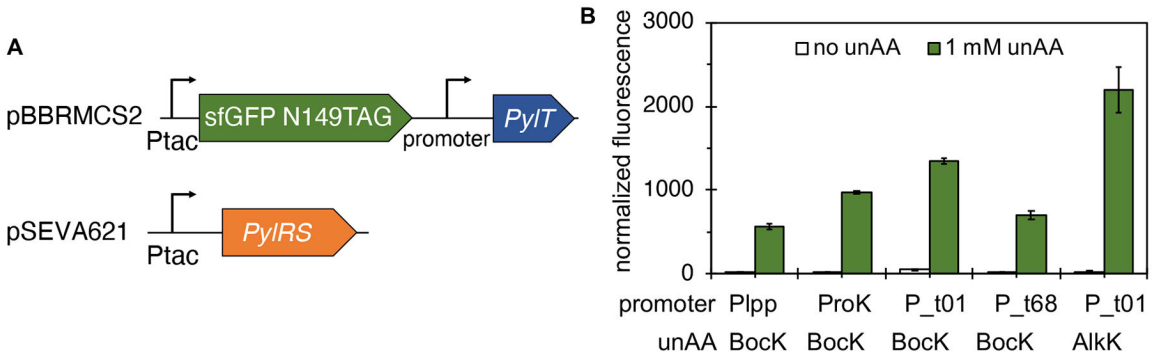

Figure 3. Genetic code expansion using the *Mb*PylRS/PylT pair in *P. putida* KT2440.

(A) Plasmid constructs for the expression of PylT and an unAA-specific *Mb*PylRS variant. Promoter for PylT was Plpp, ProK, P_t01, or P_t68. (B) Fluorescence of KT2440 cells co-transformed with pBBR-sfGFP N149TAG-PylT and pSEVA621-PylRS* or pSEVA621-AlkKRS. Fluorescence intensity was normalized to cell growth. Data is plotted as the mean ± s.d. from n= 3 independent experiments.

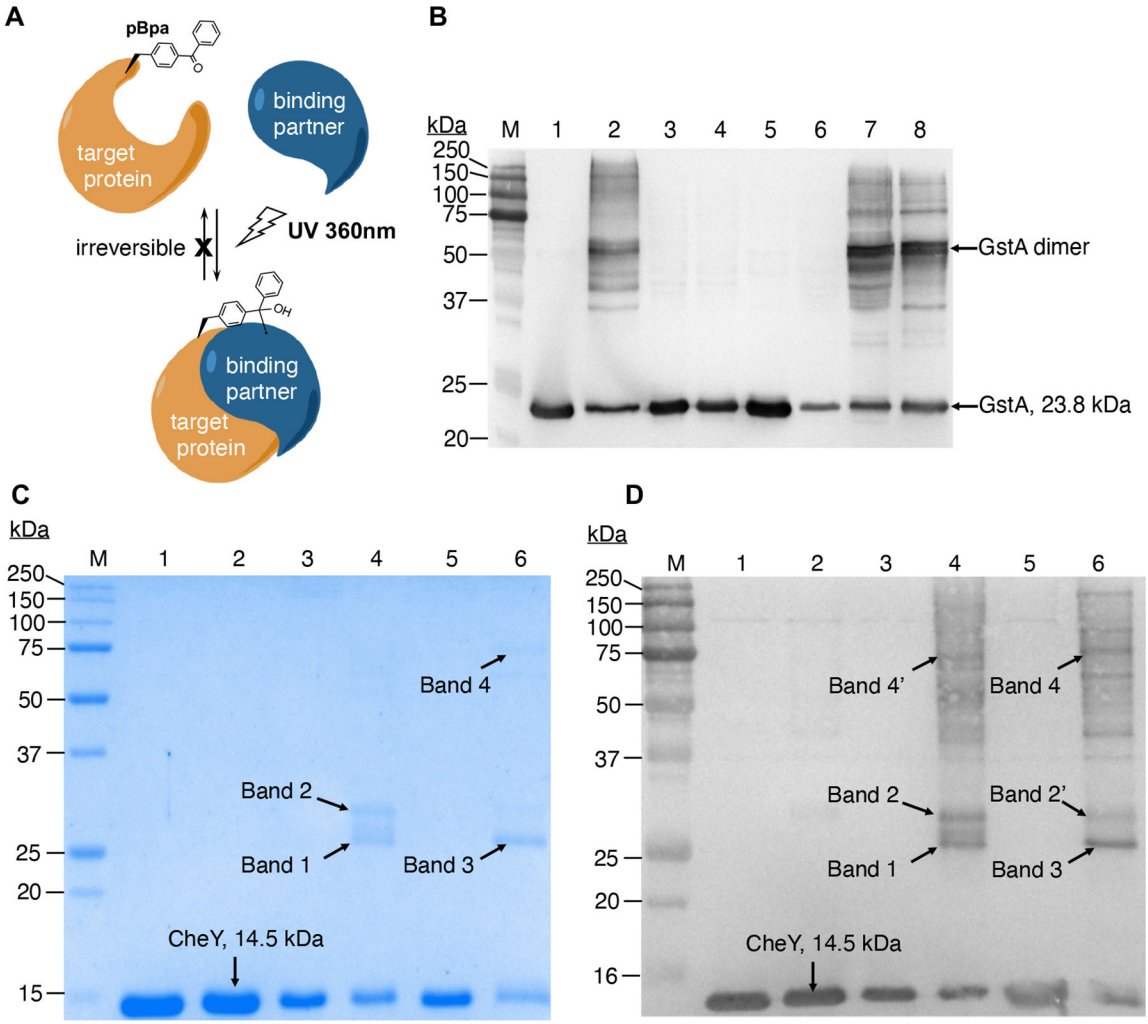

Figure 4. Detecting protein-protein interactions through pBpa-enabled photocrosslinking in KT2440.

(A) A general scheme of protein photocrosslinking using pBpa. (B) Western blot to detect dimer formation of GstA. M, protein size marker. Lanes 1 and 2, purified wild-type GstA (1) or GstA 53pBpa (2) after UV irradiation. Lanes 3 and 4, lysate of cells expressing the wild-type GstA before (3) and after (4) UV irradiation. Lane 6 and 7, lysate of cells expressing the GstA 53Bpa before (6) and after (7) UV irradiation. Lane 5 and 8, affinity purified fraction from lysate of UV-irradiated cells expressing the wild-type GstA (5) or GstA 53Bpa (8). (C) and (D) Photocrosslinking study of CheY protein in KT2440. SDS-PAGE of proteins purified by affinity resin from KT2440 (C). Western blot of proteins purified by affinity resin (D). CheY in crosslinked or unreacted form was detected by an anti-His tag monoclonal antibody. In both (C) and (D), M, protein size marker. Lane1, wild-type CheY, no irradiation; 2, wild-type CheY, irradiation at 360 nm for 30 min; 3, CheY 91pBpa, no irradiation; 4, CheY 91pBpa, irradiation for 30 min; 5, CheY 101pBpa, no irradiation; 6, CheY 101pBpa, irradiation for 30 min.